G95799 RAPPORT - BERICHT

CO 232/84

H.J. SCHÄFER

Study of high-speed combustion flows by laser velocimetry

Saint-Louis, 26.10.1984

L'auteur
Der Verfasser

H.J. Schäfer

Dr. H.J. SCHÄFER

Les Directeurs
Die Direktoren

Meunier

Ingénieur Général
R.M. MEUNIER

U. Vogel

Dr. U. VOGEL

Expl. N° 68

Ce document contient 14 + XV pages
Diese Arbeit enthält 14 + XV Seiten

Presentation given during
a visit to NASA Langley Research Center,
Hampton (Virginia/USA), 5 October 1984

<u>Key-words</u>

Combustion chambers
Laser anemometer
Velocity measurement
Correlation
Experimentation
Measurement procedures
Experimental data
Fluid mechanics

Table of contents

Introduction

Over the last decade the Franco-German Research Institute ISL at Saint-Louis, France, has been conducting research on the structure of turbulent free jets and particularly on the understanding of noise generation in jets.

The understanding of jet noise has been improved considerably since the apparent role of coherent structures in the noise producing process became evident. Since then, many authors have identified coherent structures in free jets, thereby using various measurement techniques. At ISL the investigations were concentrated on analyzing the velocity fluctuations by means of laser velocimetry and relating the results to the acoustic emission of the jet.

It was within the framework of this research program that an experimental study of high-speed combustion flows has been started. This study was primarily aimed at demonstrating the feasibility of laser velocimetry in a high-temperature jet rather than at providing a detailed description of its turbulence structure.

The main objectives were to overcome the particular problems encountered in a combustion flow and, moreover, to compare the measurement results with those found previously in an isothermal free jet. In addition to the usual information on mean and fluctuating velocities the measurements should be capable of providing the spectrum of the velocity fluctuations as well as their space-time correlation.

According to the above, this paper will be devided into three main sections :

1 - test facility and particular problems encountered in the high-temperature jet ;

2 - how we, at ISL, tried to overcome the problems ;

3 - some experimental results to demonstrate the capabilities of the measuring technique.

Hot free jet facility

The experiments were carried out with the hot free jet facility of ISL. The centre piece of this facility is a combustion chamber, which is a model of an aero-engine combustor. In this combustion chamber a fuel-air mixture is burnt and the resulting gases are expelled through a convergent nozzle. The exit diameter of the nozzle is 80 mm. Between the combustion chamber and the nozzle a 400 mm long duct is located such that a good mixing and stabilization of the flow can occur before it enters the nozzle.

For the measurements described here, the mass flow rate was kept at 0.56 kg/s resulting in an efflux velocity of about 400 m/s. The exit plane temperature was about 1200 K and the Mach number 0.6.

Experimental problems

When trying to use a laser Doppler velocimeter for measurements in a combustion flow, a number of particular problems have to be considered which are usually not present in isothermal flows. The principal problems are :

- the hostile environment with high noise and high vibration levels,
- a non-isotrope and fluctuating refractive index,
- the need for appropriate seeding.

In addition, particular requirements are to be met by the signal processing and data acquisition system :

- high speed and high accuracy,
- capability of providing spectral information,
- capability of identifying coherent structures.

Laser Doppler velocimeter

The requirements to be met by the laser velocimeter are far beyond the capabilities of commercial systems. It has therefore been necessary to select the most suitable optical layout and to develop an appropriate signal processing to produce meaningful results in the rigorous environment of the combustion chamber. For reasons of improved signal-to-noise ratio, ease of alignment, and relatively high stability against vibrations, a one-component fringe mode laser velocimeter with forward-scatter collector optics was used.

A schematic drawing of the optical arrangement is shown in figure 1 : an argon-ion laser emitting about one watt at the 515 nm wavelength is utilized. The beam is split into two parallel beams which pass through acousto-optic modulators (Bragg cells, B). These modulators have separate driving units and allow frequency differences between the beams of 2, 5 and 10 MHz to be obtained. The beams are brought to intersection by lens L_1. With the aid of mirrors S_1, S_2 and S_3 the beams are directed towards the jet flow. The interference fringes in the probe volume are oriented for the measurement of the axial velocity component.

The receiving optics is conventional, consisting of a collecting lens R_A, a narrow-band filter, and a photomultiplier. The remaining parts of the receiving optics will be discussed later in connection with the cross-correlation measurements.

The laser and the vibration-sensitive part of the transmission optics are protected from the noise originating from the combustion system by means of a protective housing. This has been found indispensible since the noise level under operating conditions can exceed 140 dB.

Precise positioning of the probe volume at a desired point in the flow is provided by a traversing system based on a hydraulic x-y table. Receiving and transmitting optics including the laser are fixed to a common mount and traversed as the whole. In order to obtain various downstream station measurements in the flow field the free jet assembly can be moved along its centre-line. The motion of the hydraulic table and the free jet assembly is controlled remotely by linear potentiometers providing an electrical read-out of the probe volume position in the x, y and z direction.

<u>Influence of refractive index fluctuations on the measurement accuracy</u>

As indicated above, it is of interest to examine the extent to which fluctuations in the fringe system may affect the measurement accuracy when temperature-dependent variations of the refractive index occur in the flow. In fact, refractive index gradients appearing normally to the propagation direction of the laser beams are capable of causing the two beams to deviate from their initial direction. This may result in changes in the position of the control volume relative to the flow as well as in variations of the fringe spacing.

The shift of the measuring point can generally be neglected as compared to the finite extension of the control volume. Variations of the fringe spacing, however, can simulate an increased turbulence of the flow and may give rise to erroneous conclusions concerning the spectrum of the velocity fluctuations.

Since a theoretical treatment of these effects is scarcely possible, an extensive experimental study has been carried out with the objective of determining the fluctuations in a fringe system which is generated in a hot supersonic flow.

In order to detect the fluctuations seen by an individual scattering particle when passing through the control volume, a time resolution in the order of 25 nano-seconds was necessary. This resolution was achieved by using a high-speed streak camera with rotating mirror.

Figure 2 shows a small section of a typical recording of the fringe pattern : the length of this section corresponds to a time interval of approximately 8 µs ; the fringe spacing is 70 microns. The picture shows the wave-like displacement of the interference fringes as a function of time.

In order to determine quantitatively the influence of these fluctuations on the accuracy of the LDV measurements, the variation in the fringe spacing was measured for a certain number of fringes and 100 particle trajectories such as indicated on the recording by the oblique white lines. These lines correspond to the space-time curves of particles traversing the control volume with the flow velocity of about 720 m/s.

As a result of an extensive evaluation of the recordings we conclude that the variation coefficient of the fringe spacing, even in the worst case, does not exceed 2,8 %. According to this result, the measured turbulence intensity can be corrected for the effects arising from the refractive index fluctuations.

The mode of correction is explained in figure 3 : provided that the velocity fluctuations and the refractive index fluctuations are not correlated, the corrected or "true" turbulence intensity τ_{corr} is given by the relation seen on the upper left of the diagram, where τ means the measured turbulence intensity and τ_d the variation coefficient of the fringe spacing.

The figure shows a plot of the turbulence correction $\Delta\tau$ and the true turbulence intensity τ_{corr} as functions of the measured turbulence intensity τ.

Considering the experimental situation, i.e. turbulence intensities that are in excess of 8 %, this correction is seen to have no practical meaning as, even in the worst case, it is only 0,5 % or, in other words, the turbulence intensity τ drops from 8 % to 7,5 %.

Seeding

Since the concentration of natural scattering particles was too low to get sufficient data rates, the flow had to be seeded artificially. This was done in the total air supply upstream of the combustion chamber using a cyclone particle generator (figure 4). The seed material was a mixture of titanium dioxide and fumed silica ("Aerosil") which had proved to be a good seeding agent earlier. The mean diameter of the titanium dioxide particles was found to be smaller than 0,5 µm. The addition of silica particles has been deemed necessary in order to prevent the titanium dioxide particles from agglomerating.

Signal processing and data acquisition

The electrical signal from the photomultiplier was processed with a counter-type LDV processor the detailed description of which has been given elsewhere. This processor, developed at ISL especially for high-speed applications, combines high accuracy and high sampling rate. It is based on zero crossing detection in individual bursts and employes end-of-burst detection for data validation. Rejection of high amplitude signals is used to minimize bias errors due to particle lag.

A block diagram of the data acquisition system is shown in figure 5. The signal processing equipment is composed of the photomultiplier tube with preamplifier, a computer-controlled frequency filter, the fore-mentioned LDA processor, a 1 MHz clock, and a digital multiplexer. To attain maximum sampling rates, the data are recorded using direct memory access to a minicomputer. The minicomputer not only provides data acquisition and reduction but also controls the frequency filter bank consisting of 8 low-pass and 8 high-pass filters. The filter bank is tuned automatically according to the instantaneous signal frequency. Low-pass and high-pass cut-off frequencies are thereby set to the center frequency plus and minus three times the standard deviation, respectively.

In order to incorporate time information in the signal processing, a 1 MHz clock has been added to the data acquisition system. Time information is recorded with each valid sample and a pair of velocity and arrival time is transmitted to the minicomputer. This allows the time between successive validated signals to be measured and both particle and time averages of the velocity to be calculated. Moreover, time information is needed for the determination of the turbulence spectrum. To obtain the turbulence spectral information, in a first step the autocorrelation function of the velocity fluctuations is established. Then, a Fourier transform of this autocorrelation function is performed providing an estimate of the turbulence power spectrum.

The entire data acquisition system was checked out carefully with simulated electronic signals as well as in the course of extensive investigations of cold free jets. In the velocity range considered here, the rms error of the individual velocity value was fcund to be substantially less than 0,5 %. In addition to this high accuracy, the novel data acquisition system offers high sampling rates. The minimum time interval between successive samples is as low as 10 µs according to the maximum data rate of the direct memory access. Only the high data rate along with appropriate seeding of the flow allows turbulence spectra to be measured within reasonable lengths of time.

Flow profiles

The experimental results that will be discussed here are the radial distribution of mean velocity and turbulence intensity measured at various downstream locations in the flow as well as the turbulence spectra.

Radial surveys of the mean flow velocity and the corresponding fluctuations were made at 10 axial locations ranging from 0.25 to 7 nozzle diameters (D) downstream of the nozzle exit. As an example of the results, the transverse scans at 0.5D, 1.5D, 3D and 6D are shown in figure 6. In this diagram $\bar{v}$ is the mean velocity and σ is the rms value of the velocity fluctuations, both given in m/s. x and z denominate the radial distance from the jet centre-line and the downstream location from the nozzle exit, respectively. Each of the radial profiles is the result of about 25 point measurements with 2000 individual realizations. This diagram illustrates the variation of the flow field with increasing distance frcm the nozzle.

The radial profiles exhibit a strong similarity when plotted in appropriate coordinates. This is demonstrated in figure 7 : here, the relative velocities are plotted versus the lateral jet coordinate centered at the nozzle radius and divided by the axial distance z. The diagram shows a very good collaps of the data for eight different locations in the jet, which is an indication of the consistancy of the measurements.

Spectral analysis

As mentioned before, not only mean velocities and turbulence intensities but also the spectrum of the velocity fluctuations in the hot jet could be determined owing to the capabilities of the novel data acquisition system. The objective of the spectral analysis was to find out if, similar to the results in isothermal jets, also in the hot jet the flow velocity fluctuates at a preferred frequency. Much could be learned about the noise generation if such preferred frequencies could be identified and correlated with the noise radiation of the jet.

Figure 8 shows the spectrum measured in the exhaust jet. The power spectral density is given in units of $(m/s)^2/Hz$. Indeed, this spectrum shows a preferred frequency of the fluctuations at about 1.5 kHz.

The spectral density has been averaged over several spectra where each individual spectrum was established from 3000 velocity samples. The frequency resolution is 61 Hz.

Space-time correlation

In the study of coherent structures it is of particular interest to measure the correlation that exists between the velocity fluctuations at two neighbouring points A and B in the flow. The temporal relationship between these fluctuations is given by the cross-correlation function, defined as

$$R_{AB}(\tau) = \lim_{T \to \infty} \frac{1}{2T} \int_{-T}^{+T} v'_A(t) v'_B(t+\tau) dt$$

where $v'_A(t)$ is the velocity fluctuation at measuring point A and $v'_B(t+\tau)$ stands for the time-delayed fluctuation at point B.

The cross-correlation results often are expressed in terms of the correlation coefficient

$$\rho_{AB}(\tau) = \frac{R_{AB}(\tau)}{\sigma_A \cdot \sigma_B}$$

where σ_A^2 and σ_B^2 are the variances of the fluctuations at point A and point B, respectively.

It has been shown earlier that laser Doppler velocimetry, when combined with digital correlation methods, can provide new and useful information about the turbulence structure of jets. Thus, coherent structures in an isothermal jet could be identified and characterized by their size and convection speed.

For the cross-correlation studies the conventional optical set-up had to be modified as shown in figure 9. As usual, two laser beams are brought to intersect in the flow region. The scattered light originating from the probe volume A is collected in near forward direction by the receiving optics. So far, the optical system is quite conventional. The cross-over of the two beams is then reproduced further downstream by means of a spherical mirror. The second measurement point (B) is also observed in forward-scatter direction. Thus, the cross-talk between the two probe volumes is negligible even at vanishing separation distances. The separation between A and B can be varied continuously from zero to approximately 120 mm.

The signals were processed using the burst-counter processor described above. The major units of the entire data acquisition system are shown in figure 10.

The data acquisition system is composed of an analog multiplexer, the fore-mentioned signal processor, a 1 MHz clock, a digital multiplexer, and a minicomputer. The velocity data from the two probe volumes appear alternately at the output of the signal processor. Together with each velocity sample the elapse time between successive signals is recorded. The time information is needed for the correlation analysis.

In order to attain maximum sampling rates, direct memory access to the mini-computer is used. The actual processor data rate during this study was typically 15 000 per second. At this data rate a total sampling time of 200 ms was sufficient to establish a reliable cross-correlogram.

Evidence of a coherent structure

In a first series of space-time correlation measurements the two probe volumes were located on the jet centre-line, one was held fixed at 3 diameters from the nozzle exit, the second was moved along the jet axis.

Typical correlograms obtained in this way are shown in figure 11. In these diagrams the cross-correlation coefficient ρ is plotted as a function of the delay time τ. Correlograms are shown for two different streamwise separations Δz between the measurement points. The sinusoidal appearance of the correlograms reveals the presence of a coherent structure which means that a certain phase relationship of the velocity fluctuations is maintained over a considerably long time.

The period of oscillation of the correlation curves gives a measure of the preferred frequency at which the flow velocity is fluctuating. The present measurements yielding a preferred Strouhal number of 0.3 are in good agreement with a previous spectral analysis.

Size of the coherent structure

Figure 12 illustrates how the correlation curves vary with the separation distance between the probe volumes. In this diagram we have summarized a series of correlograms. It shows clearly that, as the separation Δz is increased, the correlation curves and their peaks move to greater time delay. At the same time, the peak correlation coefficient decreases.

The relatively slow decay of the peak correlation with increasing separation reveals a considerably long lifetime of the coherent pattern. According to figure 12 the lifetime must be in excess of 400 µs.

The spatial extent of the coherent structure can also be deduced from the decay of the peak correlation. This is illustrated in figure 13 : here, the peak cross-correlation has been plotted over the streamwise separation between the probe volumes A and B (the correlation coefficients have been normalized to unity at zero separation). If one defines the coherence length of a structure as the separation distance after which the peak correlation drops below the fraction 1/e, the streamwise coherence length is found to exceed 1.5 nozzle diameters. This result is in good agreement with similar measurements in an isothermal jet.

Convection velocity

In addition to the size of the structures the velocity at which they are convected downstream can also be obtained from the cross-correlation measurements. The convection velocity is given by the ratio of the spacing Δz and the time delay to reach maximum correlation : $v_c = \Delta z \; / \; \tau_m$.

Figure 14 shows the centre-line distribution of the convection velocity. The crosses are the values obtained from the correlograms; they are plotted against the streamwise distance from the nozzle. The convection velocity rises with the distance z and then approaches the mean flow velocity which has been plotted for comparison (broken curve).

Again, a reasonable agreement with the measurements in an isothermal jet is found. This is demonstrated in figure 15. Here, the convection speed has been non-dimensionalized by the local mean flow velocity $\bar{v}$. The crosses are the measured values for the hot jet, the dashed line represents the measurements for the cold jet. The slopes of the straight lines are slightly different, but this difference vanishes if the distance z is normalized by the potential core length of the respective jet.

Conclusions

The present experiments have shown that the particular problems encountered in a combustion flow can be overcome if a carefully designed optical set-up as well as an appropriate signal processing and data acquisition system is used. In this way, laser Doppler velocimetry can provide new and useful information about coherent structures in hot free jets. The measurement results are shown to be in good agreement with previous measurements in an isothermal jet.

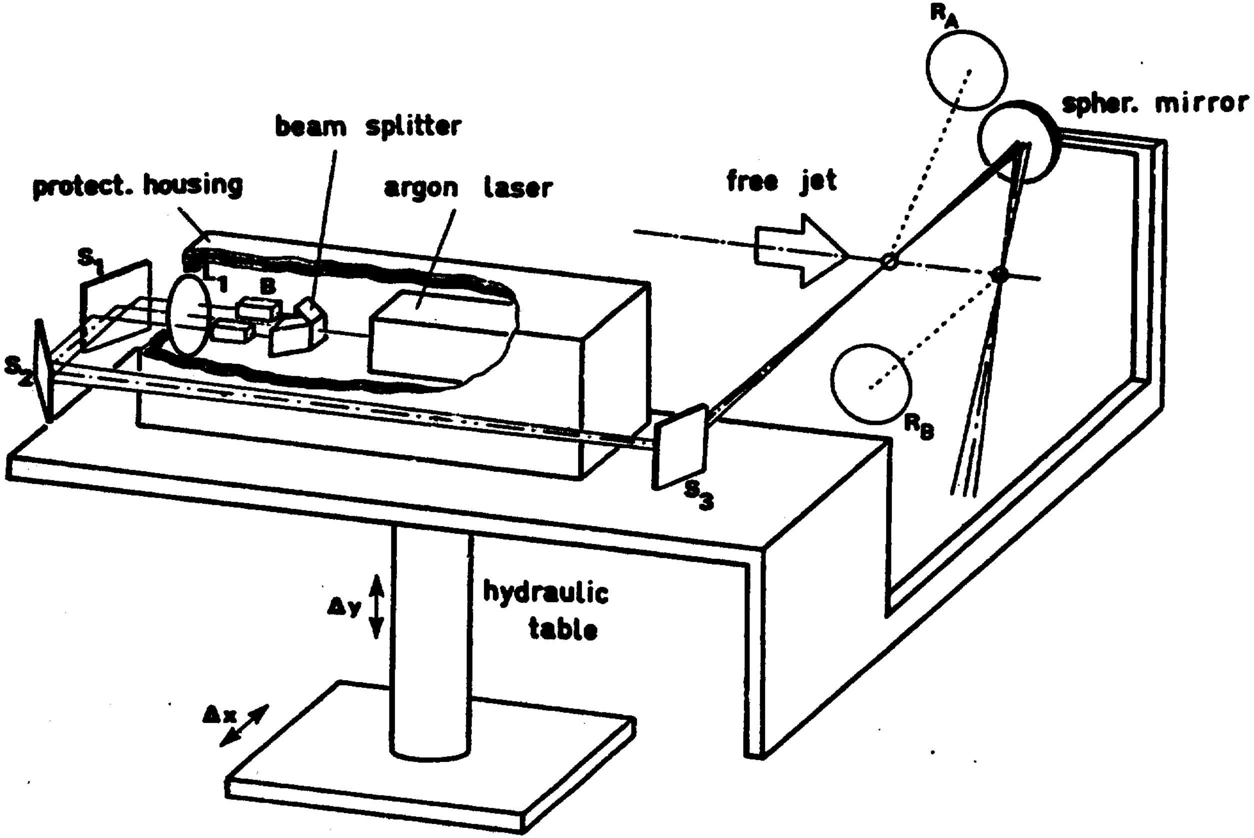

Fig.1 : Optical set-up for the LDV measurements

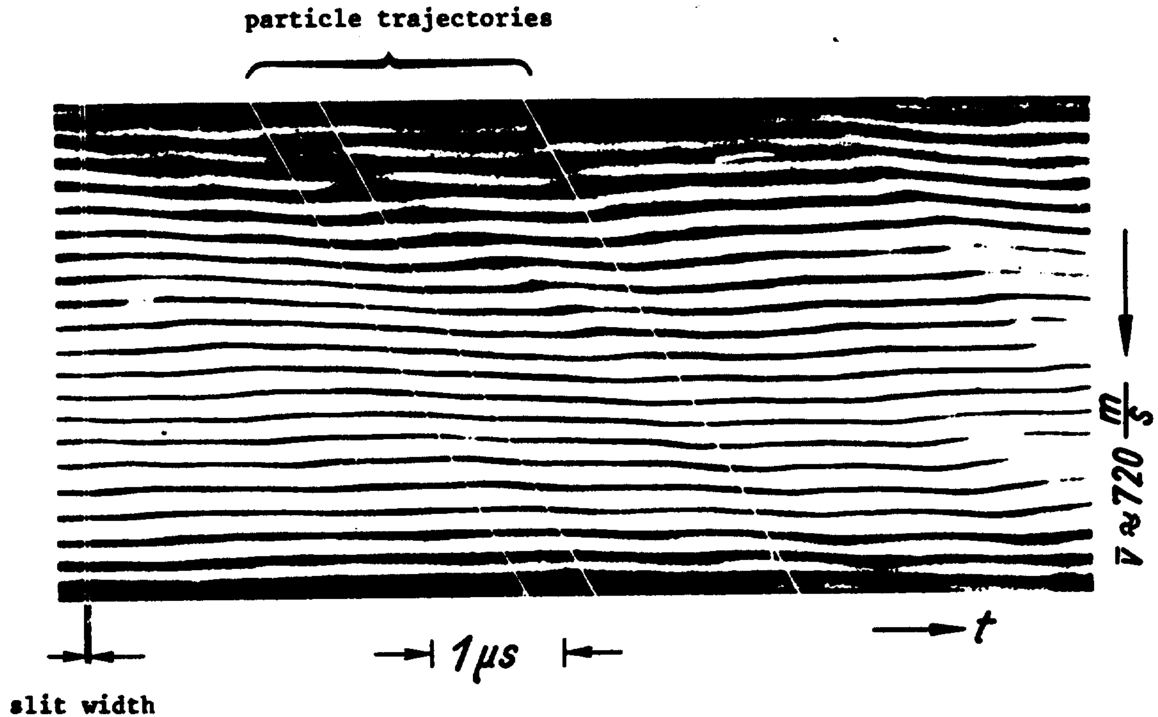

Fig.2 : Recording of the fringe pattern fluctuations in a high-temperature supersonic jet

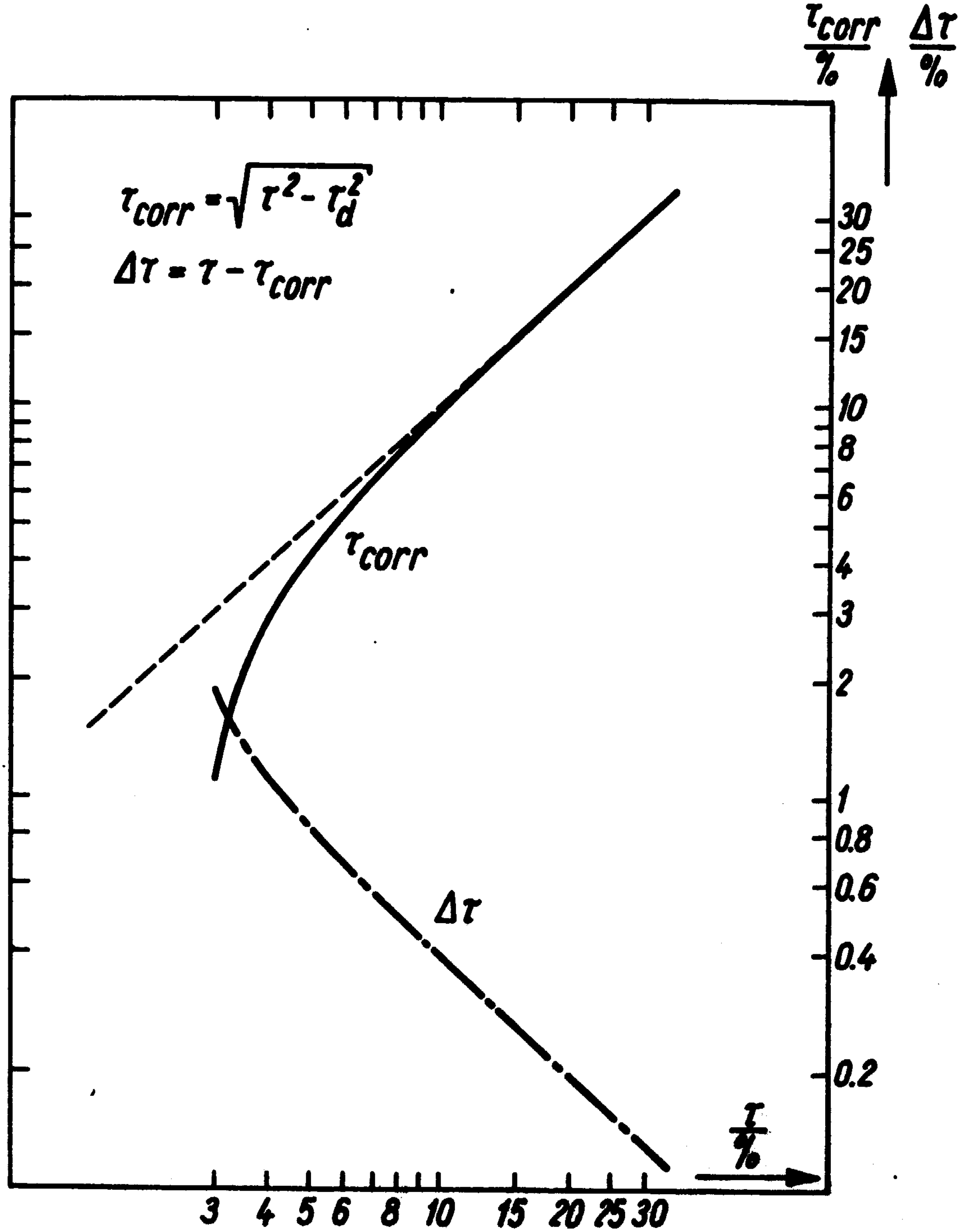

Fig.3 : Turbulence correction for effects of fringe pattern fluctuations

Fig.4 : Schematic diagram of the solid particle generator

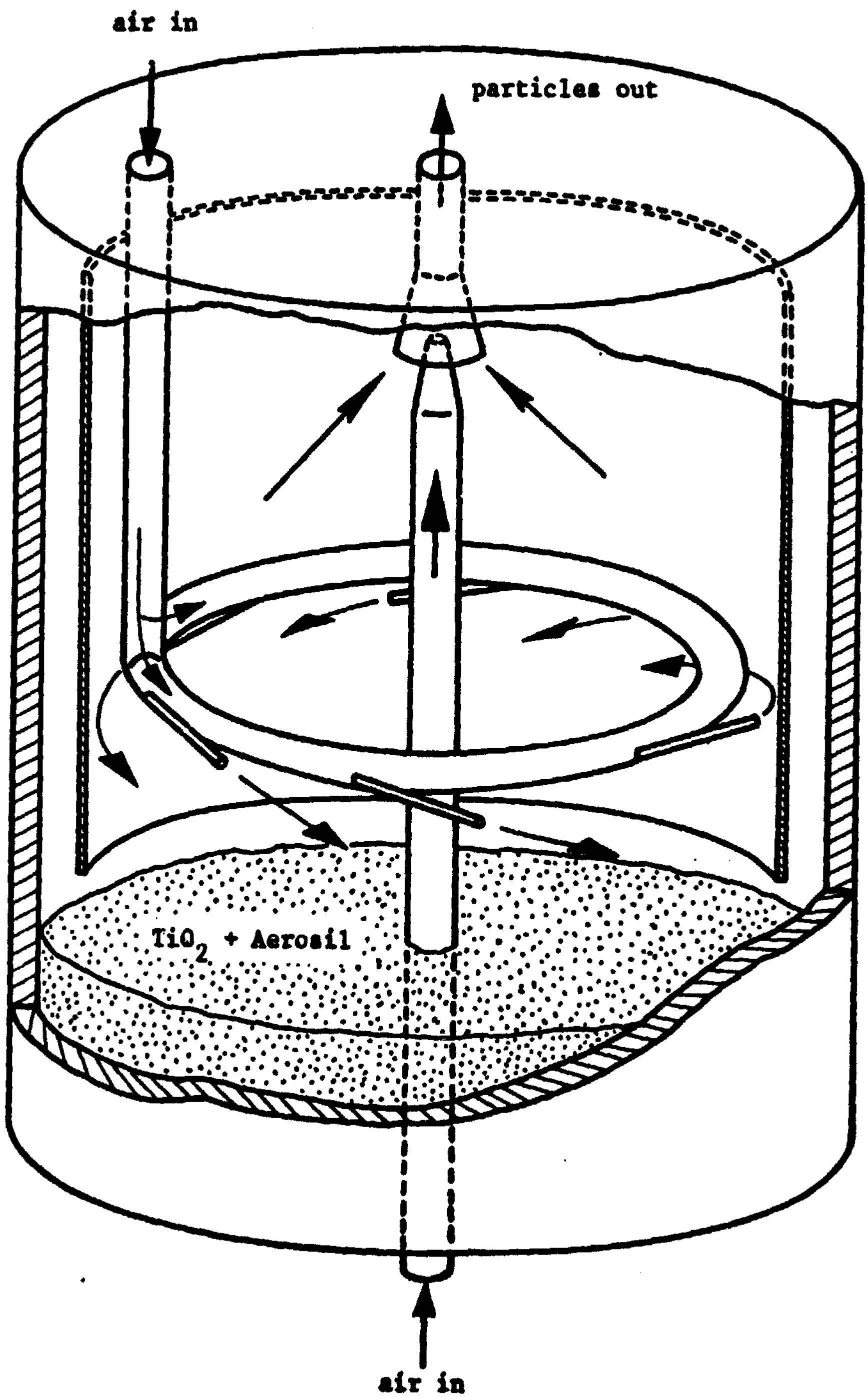

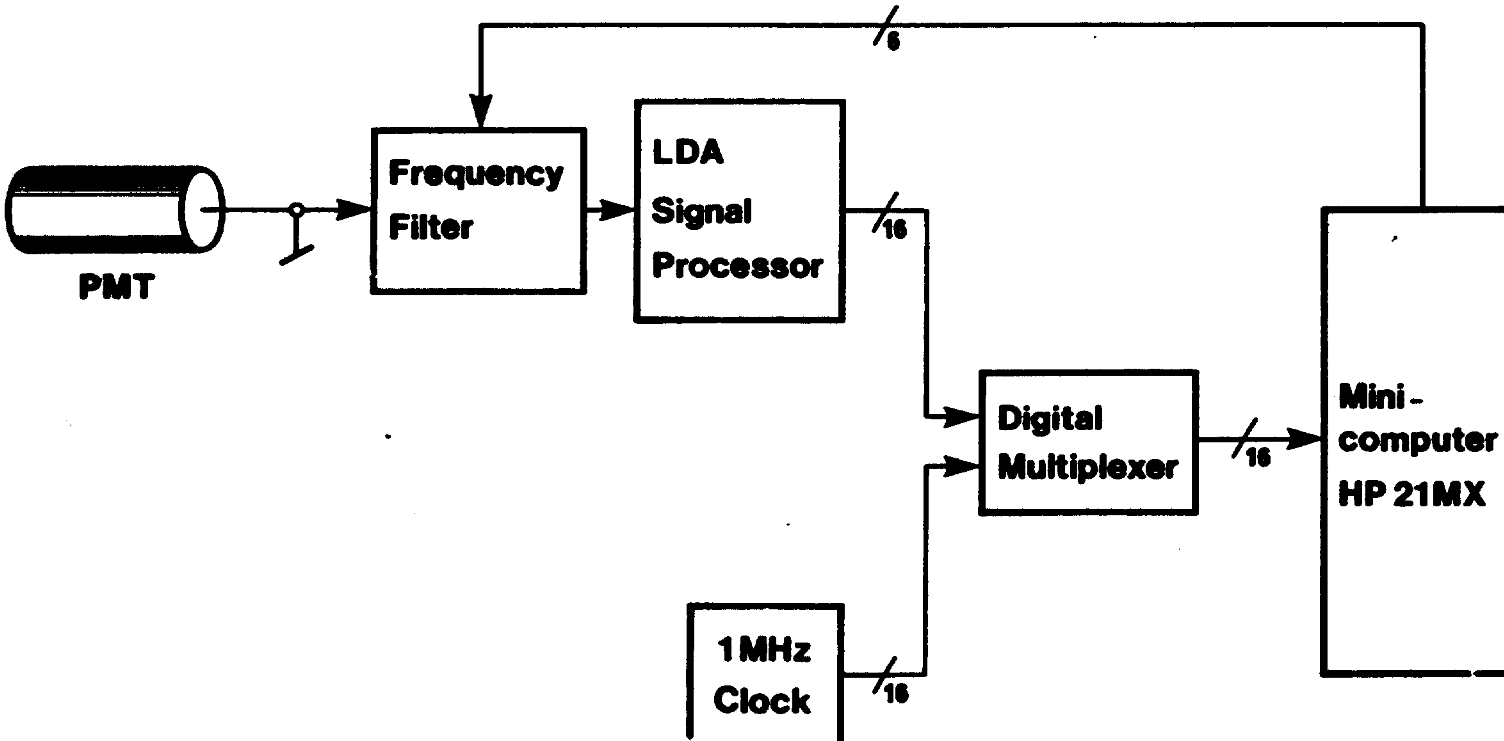

<u>Fig.5</u> : Data acquisition system for velocity and spectral measurements

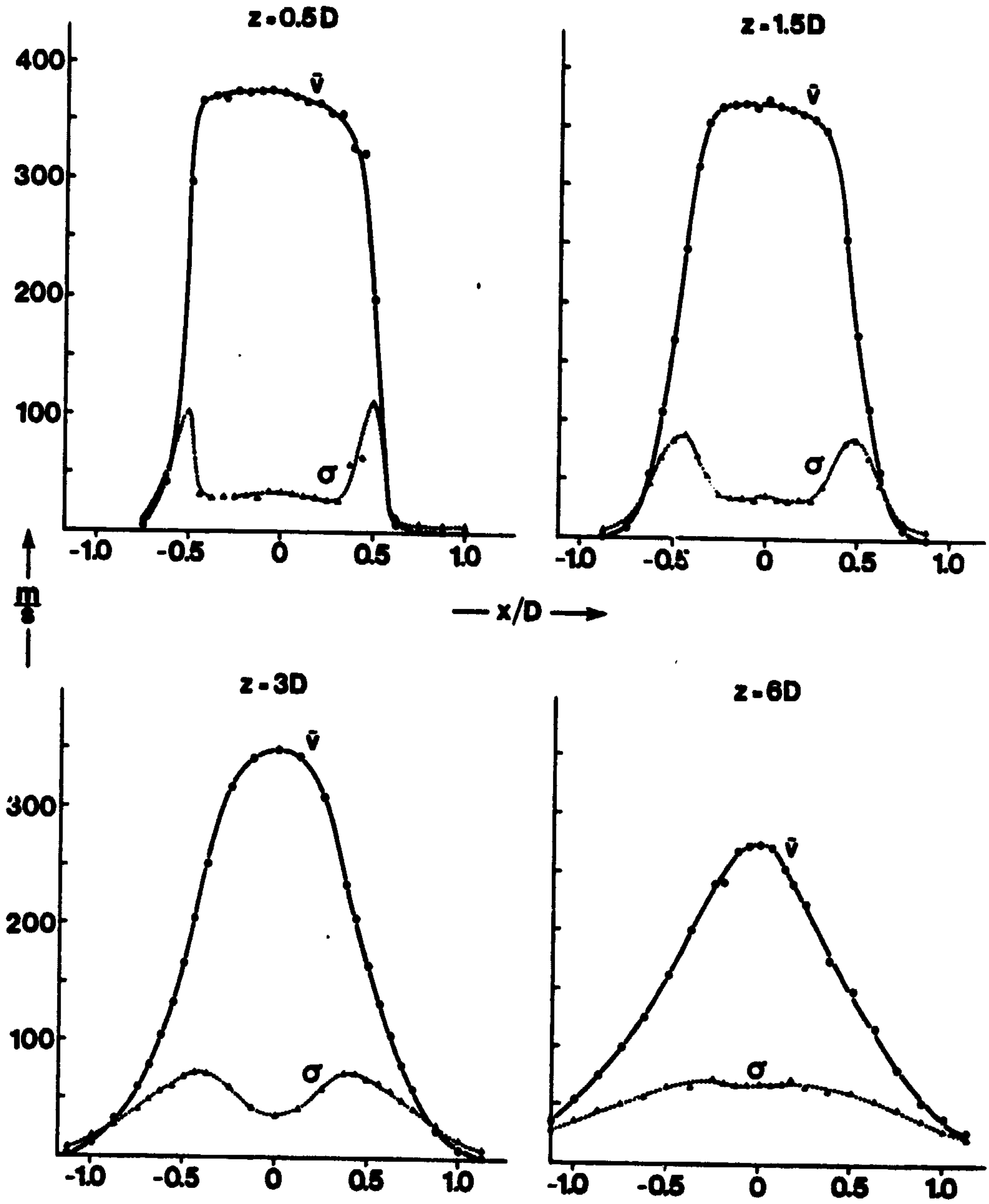

Fig.6 : Flow profiles of the hot free jet

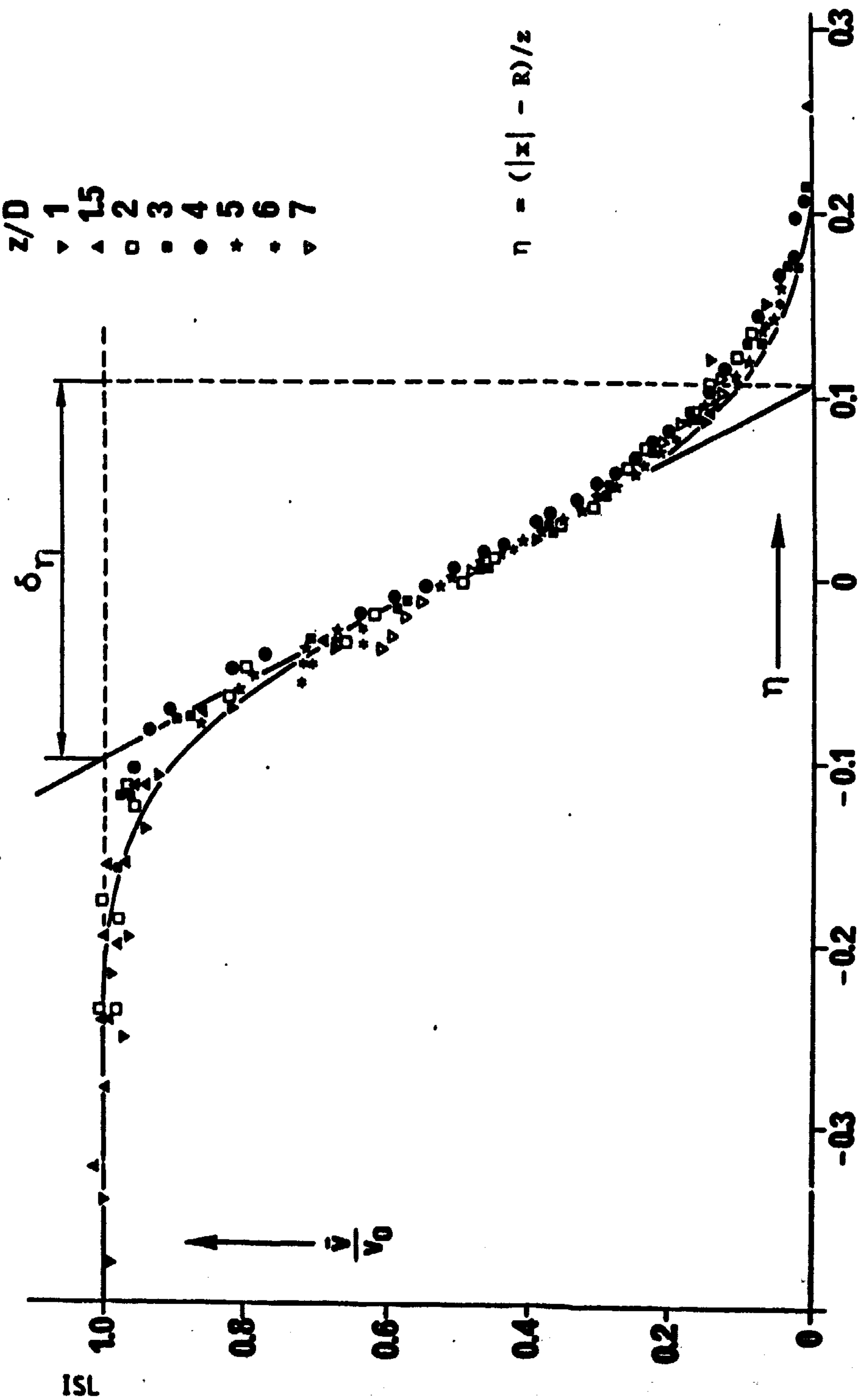

Fig.7 : Normalised velocity profiles (on similarity coordinates)

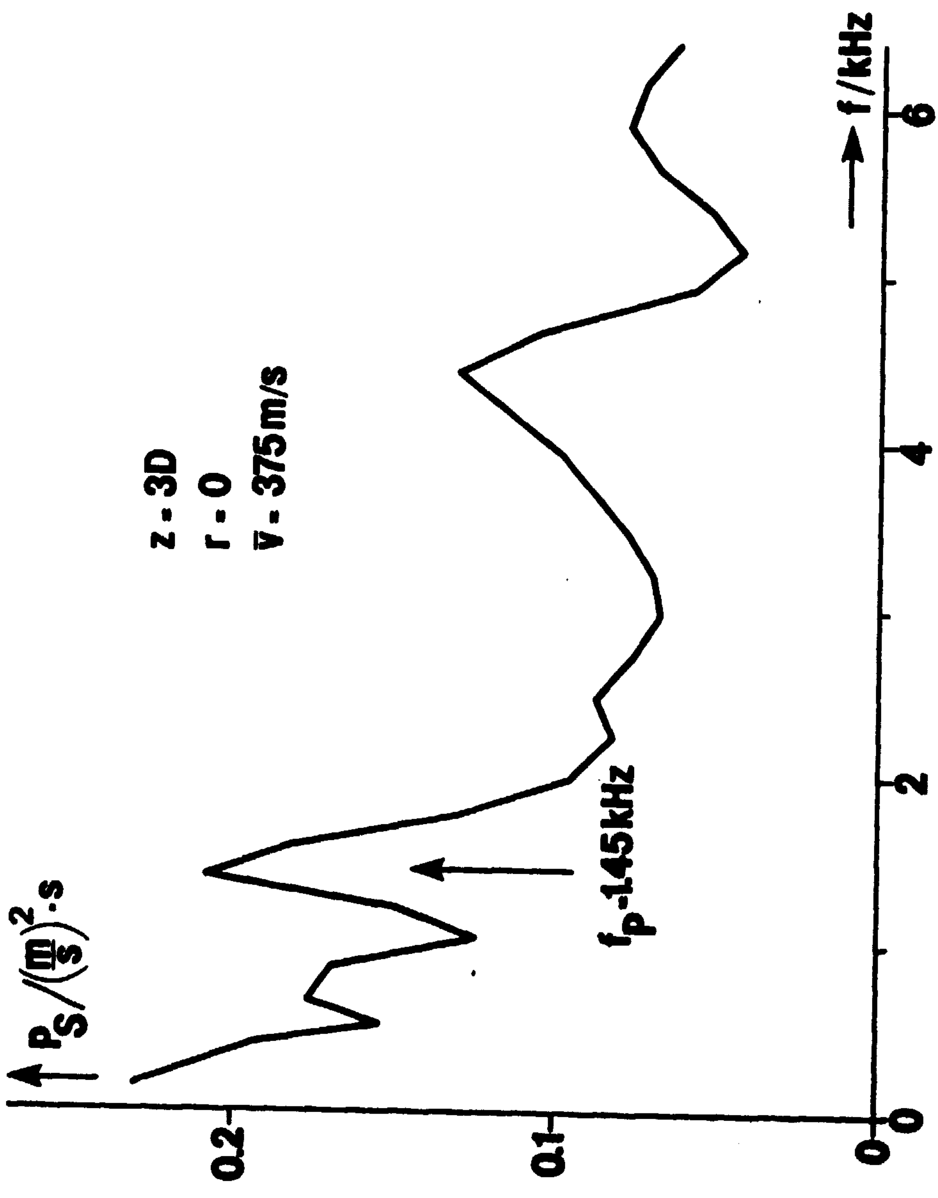

Fig.8 : Power spectrum of the velocity fluctuations

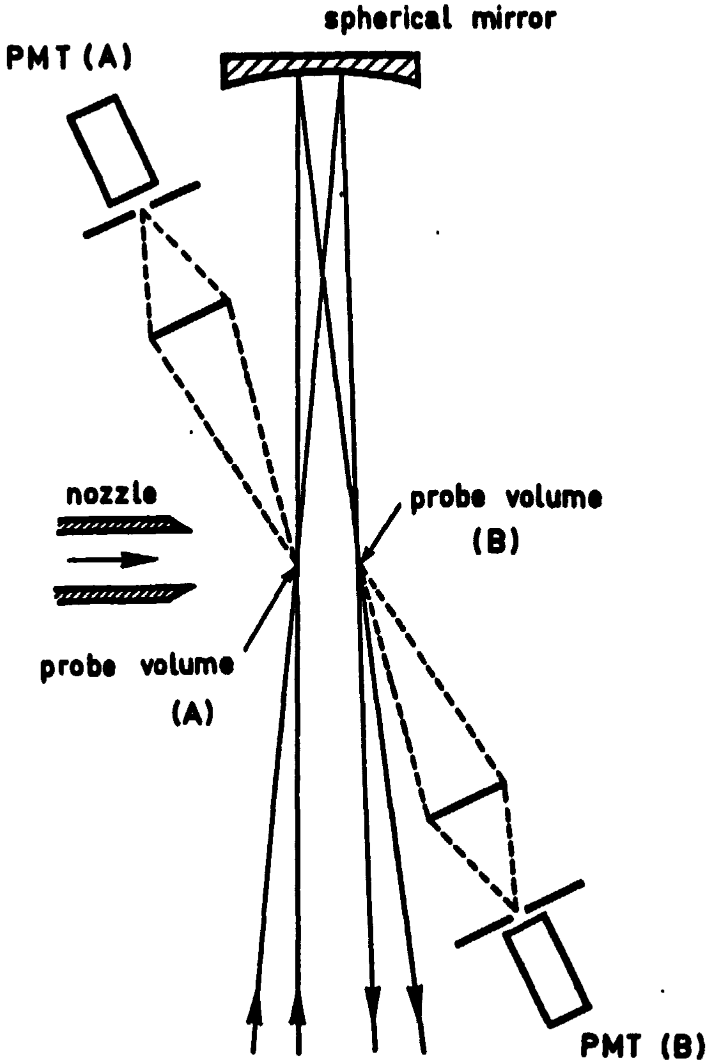

Fig.9 : Optical arrangement for cross-correlation measurements

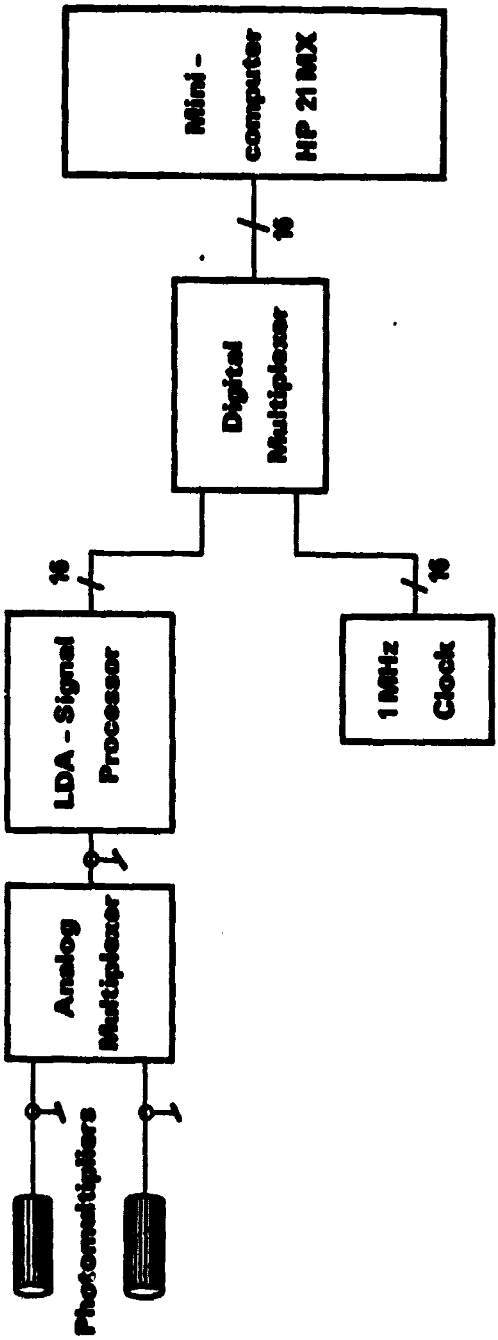

Fig. 10 : Data acquisition system for cross-correlation measurements

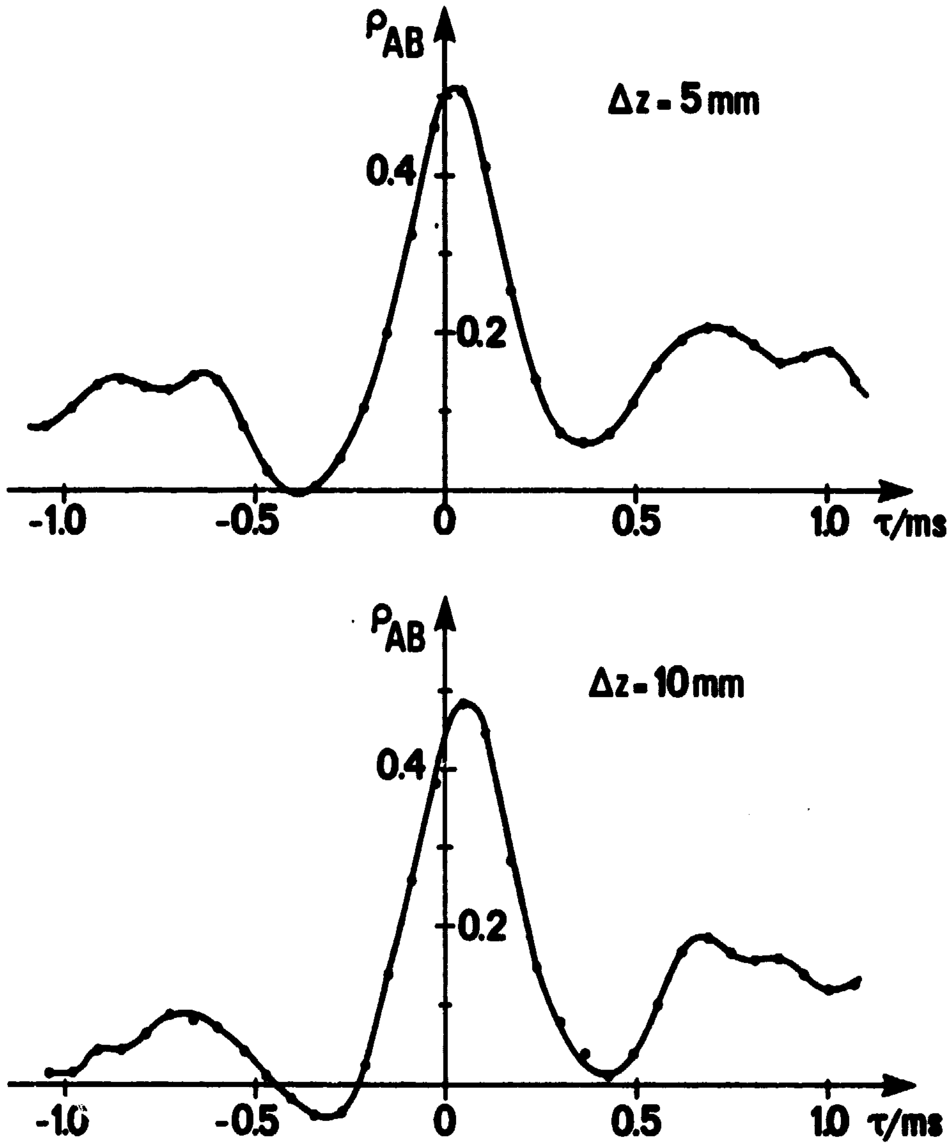

Fig.11 : Typical cross-correlograms

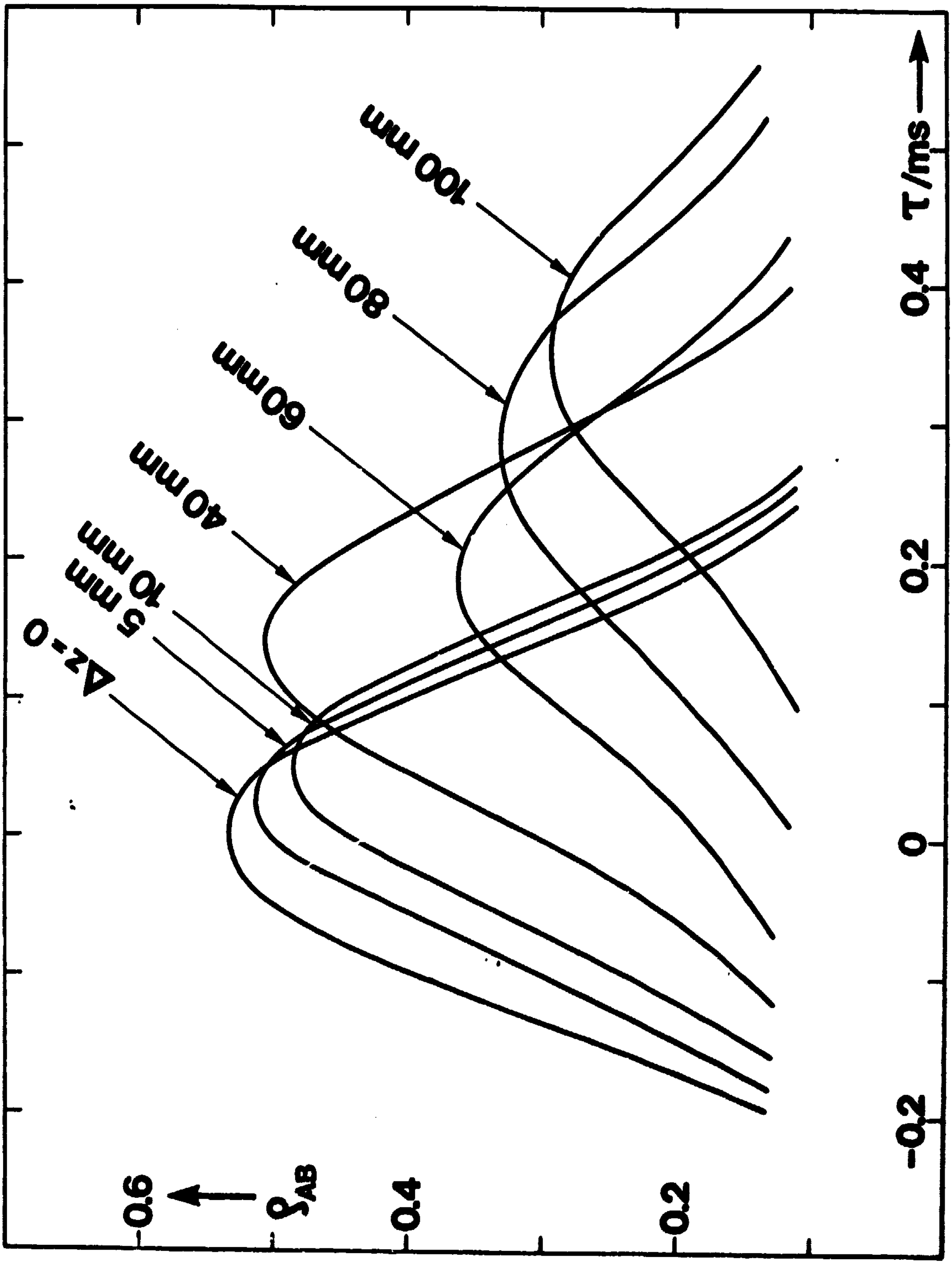

Fig.12 : Variation of the cross-correlograms with the streamwise separation of the probe volumes

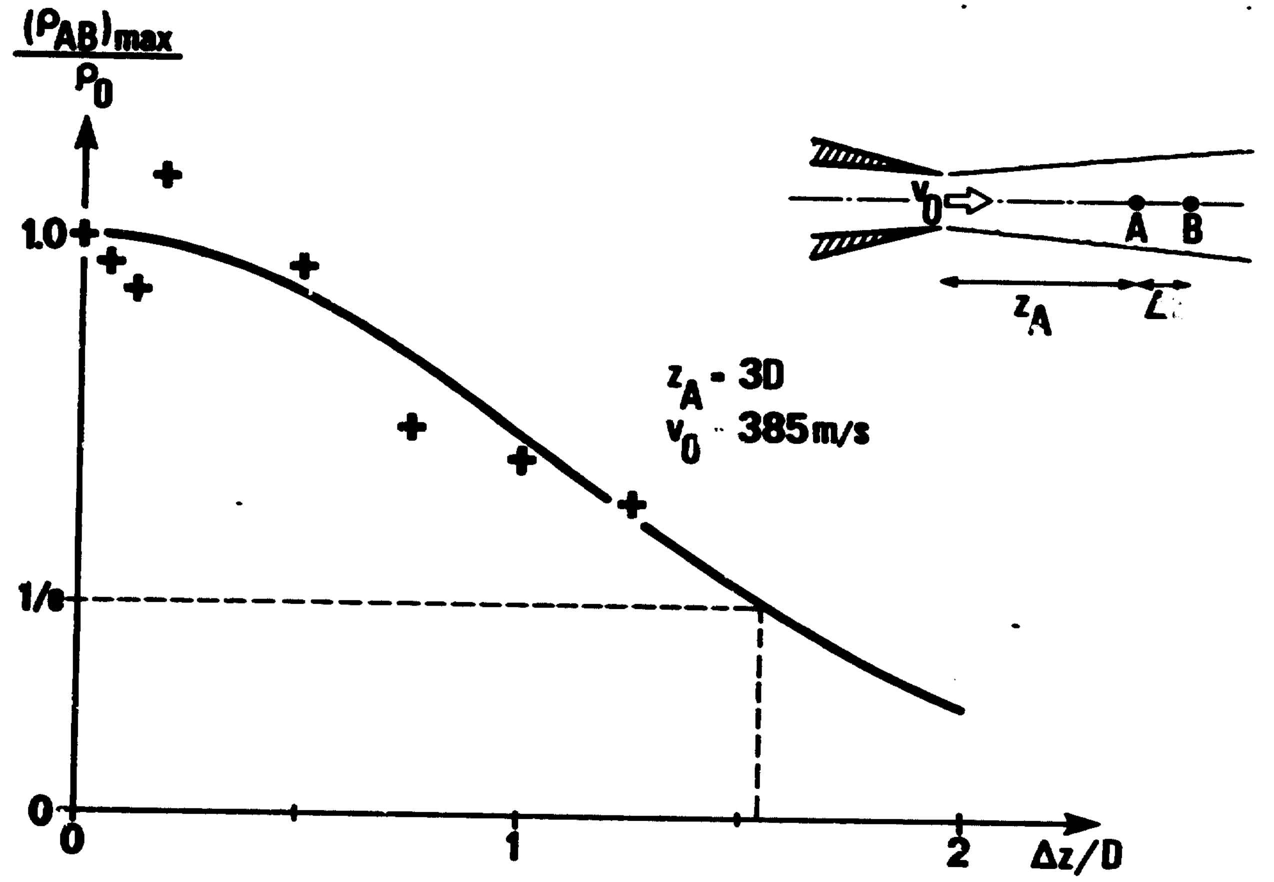

Fig. 13 : Maximum cross-correlation coefficient as a function of the probe volume separation

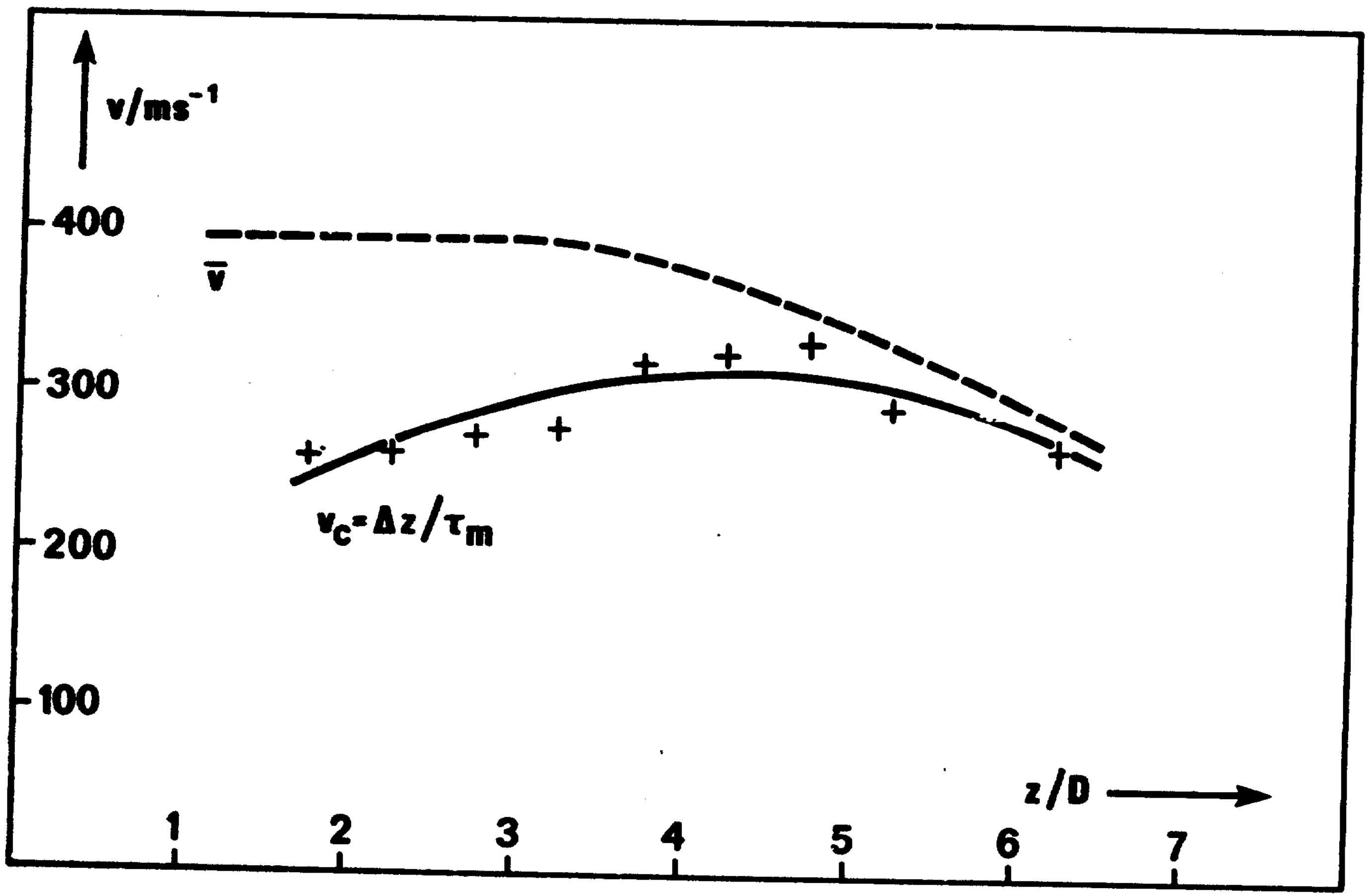

Fig.14 : Centre-line distribution of the convection velocity v_c and the mean flow velocity $\bar{v}$

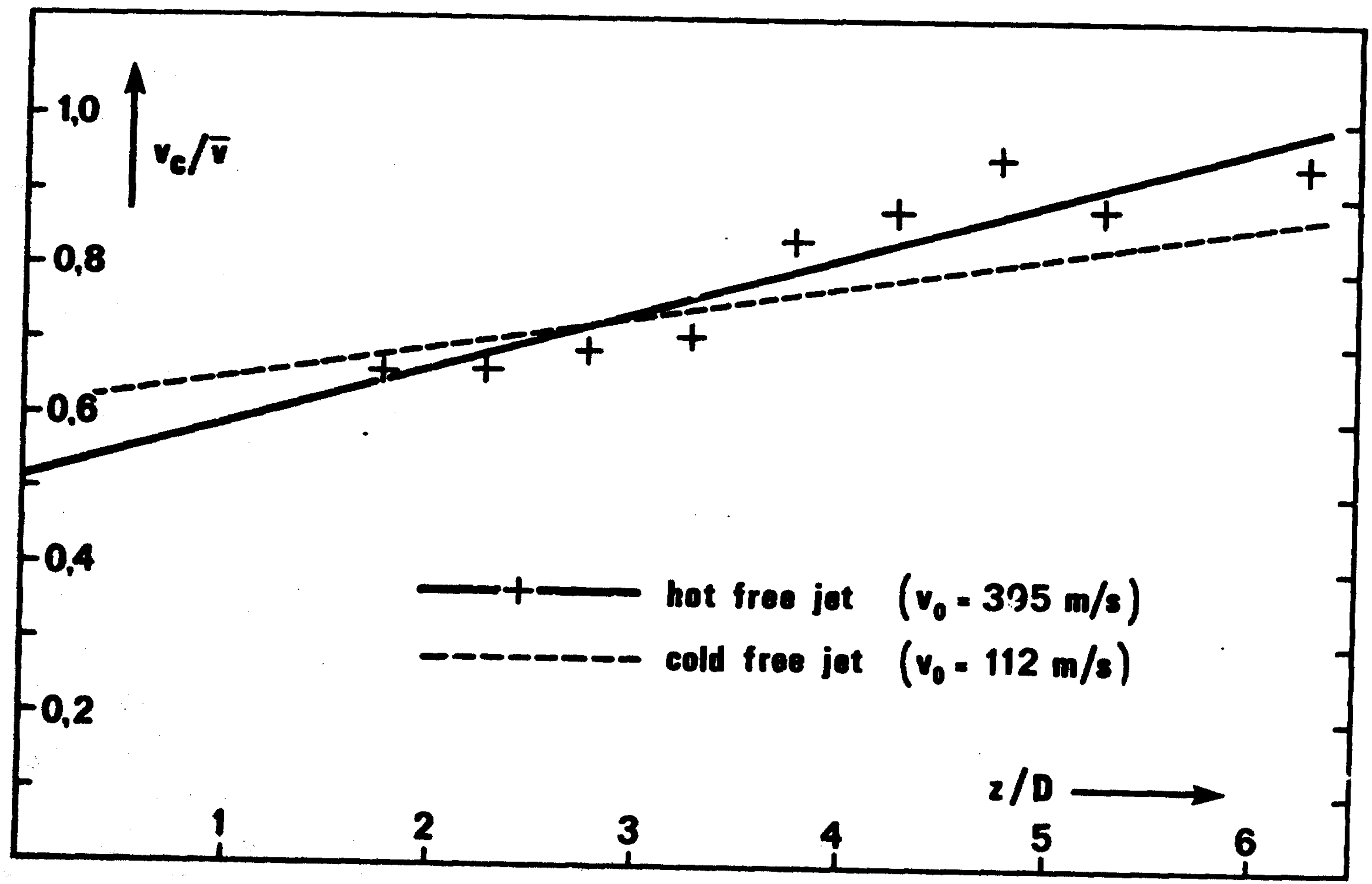

Fig.15 : Relative convection velocities in a hot jet (present work) and a previously measured isothermal jet